Journal of Crystal Growth 582 (2022) 126520

Contents lists available at ScienceDirect

Journal of Crystal Growth

journal homepage: www.elsevier.com/locate/jcrysgro

Effect of high temperature homoepitaxial growth of β-Ga_2O_3 by hot-wall metalorganic vapor phase epitaxy

Kazutada Ikenaga [a,b], Nami Tanaka [a], Taro Nishimura [a], Hirotaka Iino [c], Ken Goto [a], Masato Ishikawa [d], Hideaki Machida [d], Tomo Ueno [c], Yoshinao Kumagai [a,e,*]

[a] Department of Applied Chemistry, Tokyo University of Agriculture and Technology, Koganei, Tokyo 184-8588, Japan
[b] TAIYO NIPPON SANSO CORPORATION, Minato-ku, Tokyo 108-0014, Japan
[c] Department of Electrical and Electronic Engineering, Tokyo University of Agriculture and Technology, Koganei, Tokyo 184-8588, Japan
[d] Gas-Phase Growth Ltd., Koganei, Tokyo 184-0011, Japan
[e] Institute of Global Innovation Research, Tokyo University of Agriculture and Technology, Koganei, Tokyo 184-8588, Japan

ARTICLE INFO

Communicated by Tanya Paskova

Keywords:
A1. Crystal structure
A3. Metalorganic vapor phase epitaxy
B1. Oxides
B2. Semiconducting gallium compounds
B2. Semiconducting III-VI materials

ABSTRACT

The effect of high temperature homoepitaxial growth of (010) β-Ga_2O_3 layer by low pressure hot-wall metalorganic vapor phase epitaxy was investigated. In the growth-temperature range 800–1000 °C, the growth rate decreased with increasing growth temperature and the growth mode changed from three-dimensional island growth to two-dimensional step-flow growth. At 1000 °C, a smooth, twin-free single-crystalline homoepitaxial layer with a structural quality equivalent to that of the substrate could be grown. As the growth temperature increased, the concentration of precursor-derived C impurities decreased, while that of unintentionally incorporated Si impurities increased. It was found that the grown layers were all n-type and showed an effective donor concentration approximately equal to the Si impurity concentration regardless of the C impurity concentration.

1. Introduction

Beta gallium oxide (β-Ga_2O_3), an ultra-wide bandgap semiconductor crystal with a bandgap of 4.4–4.9 eV [1,2] and a large dielectric breakdown field greater than 7 MV/cm [3,4], has been attracting attention as a candidate material for future power devices. Unlike its counterparts GaN and 4H-SiC, bulk crystals of β-Ga_2O_3 can be grown by various melt-growth methods such as edge-defined film-fed growth (EFG) [5,6], Czochralski [7,8], and vertical Bridgman [9]. Consequently, numerous research groups are currently investigating the homoepitaxial growth of β-Ga_2O_3 using various methods such as molecular beam epitaxy (MBE) [10,11], halide vapor phase epitaxy (HVPE) [12–14], mist chemical vapor deposition (mist CVD) [15,16], low pressure CVD (LPCVD) [17], and metalorganic vapor phase epitaxy (MOVPE) [18–20]. The availability of the homoepitaxial layers has accelerated research into the fabrication of various Schottky barrier diodes (SBDs) [21–24] and field-effect transistors (FETs) [25–29] using homoepitaxial layers grown by MBE [27] or HVPE [21–24,26,28,29]. Nonetheless, the growth of β-Ga_2O_3 by MOVPE is still attractive because MOVPE is generally excellent for controlling the thickness of grown layers and the composition of alloys [$(Al_xGa_{1-x})_2O_3$]; growth systems capable of growing on multiple substrates might be developed in the future.

Ga_2O_3 growth by MOVPE has long been avoided because of the violent reactivity of oxygen (O_2) with metalorganic compounds of Ga and concerns about carbon (C) contamination. Recently, however, several research groups have attempted β-Ga_2O_3 growth by their close injection showerhead MOVPE system at 700–950 °C under low pressures (20–120 Torr) using triethylgallium (TEGa) and O_2 as source gases and argon (Ar) as a carrier gas, and demonstrated the growth of high-purity n-type homoepitaxial layers with low carrier densities and high electron mobilities [19,20], although the chemistry behind the growth was not well understood. Then, some of the authors of the present paper have conducted a thermodynamic analysis of a MOVPE system using TEGa and O_2 as source gases and have clarified that TEGa-derived hydrocarbons and hydrogen (H_2) undergo complete combustion at high temperatures and with sufficient O_2 supply, resulting in β-Ga_2O_3 growth [30]. In addition, a low pressure MOVPE growth system for β-Ga_2O_3 with a hot-wall structure was constructed for controlled growth according to the thermodynamic analysis results, and it was confirmed

* Corresponding author at: Department of Applied Chemistry, Tokyo University of Agriculture and Technology, Koganei, Tokyo 184-8588, Japan (Y. Kumagai).
E-mail address: 4470kuma@cc.tuat.ac.jp (Y. Kumagai).

https://doi.org/10.1016/j.jcrysgro.2022.126520
Received 3 December 2021; Received in revised form 24 December 2021; Accepted 4 January 2022
Available online 10 January 2022

that the C and H impurity concentrations decreased as the growth temperature increased, and finally growth of smooth $(\bar{2}\,0\,1)$ oriented β-Ga_2O_3 layers without C and H contamination has been demonstrated on *c*-plane sapphire substrates at 900 °C under a low reactor pressure of 20 Torr [30]. However, since the layers were grown on a foreign substrate, the influence of growth temperature on the growth mode and the characteristics of the grown layers was not well understood.

In the present study, homoepitaxial β-Ga_2O_3 layers were grown by the low pressure hot-wall MOVPE at 800–1000 °C. Then, the effects of growth temperature on the growth behavior, structural quality, impurity incorporation, and electrical properties of the grown layers were investigated in detail.

2. Experimental

The horizontal low pressure hot-wall MOVPE system [30] used in our previous work was also used. TEGa and O_2 were used as the precursors, and Ar was used as the carrier gas. The total gas flow rate was 1100 sccm, and the pressure in the quartz glass reactor was maintained at 20 Torr throughout the entire growth process.

Undoped β-Ga_2O_3 layers were directly grown on n-type Sn-doped (010) β-Ga_2O_3 substrates (Novel Crystal Technology, Inc.) with an effective donor concentration (N_d – N_a) of 4 × 10^{18} cm^{-3} prepared by EFG. After the substrate was loaded into the reactor, it was heated to a growth temperature of 800 to 1000 °C in an Ar carrier gas containing O_2 (O_2 partial pressure of 1.0 Torr). The TEGa supply was then started, and homoepitaxial growth was carried out for 1 h. The partial pressures of TEGa and O_2 were 2.0 × 10^{-2} Torr (48.6 µmol/min) and 1.0 Torr, respectively, during the growth (corresponding to a VI/III ratio of 100). After the growth, only the TEGa supply was stopped, and the substrate was cooled to room temperature.

The thickness and impurity concentration of the grown layers were examined by secondary ion mass spectrometry (SIMS; CAMECA, IMS-7f). The surface morphology was evaluated by atomic force microscopy (AFM; SHIMADZU, SPM-9600). The structural quality was characterized by high-resolution X-ray diffraction (XRD; Spectris, X'Pert MRD) using Cu Kα_1 X-ray source. To clarify the N_d – N_a value for the grown layers, vertical SBDs were fabricated and capacitance–voltage (*C–V*) measurements (LCR meter; HEWLETT PACKARD, 4284A) were performed. The fabrication of the SBDs began with activation annealing at 1000 °C for 1 h under a nitrogen (N_2) atmosphere [6]. The back surfaces of the substrates were then chemo-mechanically polished to remove the damaged layer formed during the manufacturing process of the substrates, followed by blanket evaporation of Ti (20 nm)/Au (500 nm) and rapid thermal annealing at 450 °C for 3 min under a N_2 atmosphere to form an ohmic cathode electrode. Finally, circular Ni (10 nm)/Au (500 nm) electrodes with a diameter of 500 µm were evaporated onto the surfaces of the grown layers to form Schottky anode electrodes.

3. Results and discussion

Fig. 1 shows the temperature dependence of the homoepitaxial growth rate for the β-Ga_2O_3. For comparison, the heteroepitaxial growth rate on a *c*-plane sapphire substrate under the same conditions [30] is also plotted in the figure. The growth rates were simply obtained from the grown layer thickness after 1 h of growth. Almost no difference was observed between the rate of growth on the β-Ga_2O_3 substrate and that on the *c*-plane sapphire substrate. This observation implies that there is no incubation period for wetting layer formation on sapphire, which is often a problem in the early stages of heteroepitaxial growth of group-III nitrides on sapphire [31,32], and that there is no difference in the growth rate of the $(\bar{2}\,0\,1)$ and (010) planes of β-Ga_2O_3. In addition, the growth rate decreased from 1.6 µm/h at 800 °C to 0.9 µm/h at 1000 °C. This is typical behavior on the high-temperature side of the region where

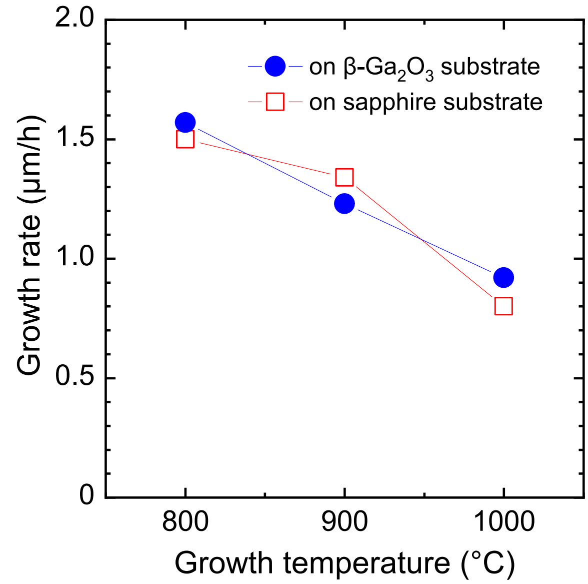

Fig. 1. Growth-temperature dependence of MOVPE growth rate for β-Ga_2O_3 on (010) β-Ga_2O_3 substrates and *c*-plane sapphire substrates.

the growth process is thermodynamically limited, that is, mass transport limits the growth. Similar results have also been reported in the literature [18,30,33].

AFM surface images of the homoepitaxial β-Ga_2O_3 layers grown at each temperature for 1 h are shown in Fig. 2. At a growth temperature of 800 °C [Fig. 2(a)], three-dimensional (3D) island growth was dominant, and numerous protrusions with an average height of ~ 25 nm were observed on the surface at a density above 10^8 cm^{-2}. However, as is evident from the root-mean-square roughness (R_{rms}) values shown in each image, the surface of the grown layer became smoother as the growth temperature was increased. For the layer grown at 1000 °C [Fig. 2(c)], the R_{rms} value decreased to 0.62 nm, and regularly spaced steps and terraces aligned approximately along the [001] direction were observed, similar to the results in Refs. [18–20]. It should be noted here that the R_{rms} value of the grown layer increased with increasing scan area, but the tendency to decrease with increasing growth temperature did not change. These results show that the two-dimensional (2D) step-

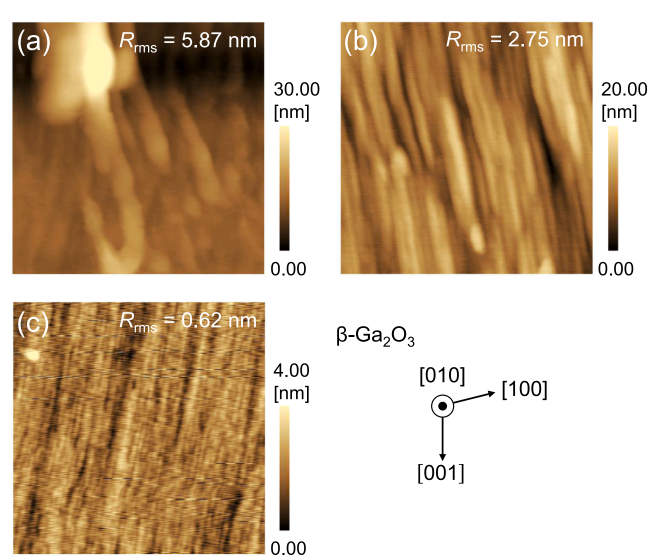

Fig. 2. AFM surface images of 1 × 1 µm^2 scanned areas of homoepitaxial (010) β-Ga_2O_3 layers grown for 1 h at (a) 800, (b) 900, and (c) 1000 °C. The R_{rms} value is shown in each image.

flow growth mode is dominant at temperatures as high as 1000 °C. In our previous report, when β-Ga_2O_3 was grown on a *c*-plane sapphire substrate, the grown layer surface became rough at a growth temperature of 1000 °C [30]. Presumably, the difference is attributable to heteroepitaxial growth on the sapphire substrate.

Subsequently, the structural quality of the homoepitaxial layers shown in Fig. 2 was evaluated by XRD. The XRD 2θ–ω mode profile for each homoepitaxial sample (data not shown) showed no peaks other than (0 2 0) plane, indicating that the grown layers were (0 1 0)-oriented following the substrate. Then, XRD {1 1 1} pole figure was measured to see if in-plane-rotated twins were formed in the grown layer with the (0 0 1) or (1 0 0) planes as the twin boundaries. The results are shown in Fig. 3. In the pole figures for samples grown at 800–1000 °C, peaks were observed only at two locations (ϕ = 126.3° and 306.3°) when ψ was 33.0°; these features are the same as those observed for the initial substrate. These results indicate that twins are not present in the homoepitaxial layers and that the layers are single-crystalline (0 1 0) β-Ga_2O_3 layers.

The structural quality of each homoepitaxial layer was further investigated using XRD ω-rocking curves. Fig. 4 shows the growth-temperature dependence of the full width at half maximum (FWHM) of the XRD ω-rocking curve for the unskewed asymmetric ($\bar{4}\,2\,\bar{2}$) plane with a low X-ray incident angle of about 1.5°. It has been reported that the penetration depth of X-ray is about 0.7 μm with this arrangement [34]. Therefore, the structural quality of only the homoepitaxial layers could be evaluated without contribution from the substrates. The FWHM values for the XRD ω-rocking curves were almost constant at 75–77 arcsec at the growth temperature of 800–1000 °C, which were almost the same as that of the initial substrate. These results show that although the grown layer surface becomes rough at 800 °C, a homoepitaxial layer with a high structural quality equivalent to that of the initial substrate (dislocation density on the order of 10^3 cm^{-2} [6]) can be grown at a growth temperature of 800–1000 °C without introducing new dislocations during the growth.

Finally, SIMS and *C*–*V* measurements were performed to investigate the $N_d - N_a$ value for the homoepitaxial layers. Fig. 5 shows the SIMS depth profiles of C and silicon (Si) impurity concentrations in the homoepitaxial β-Ga_2O_3 layers grown at each temperature. In all layers, H and N impurity concentrations were below the background (B. G.) levels of the SIMS system (1 × 10^{17} cm^{-3} for H, 2 × 10^{16} cm^{-3} for N, respectively). The homoepitaxial layer grown at 800 °C contained C and Si impurities with concentrations on the order of 10^{18} cm^{-3}, and the C concentration was higher than the Si concentration. However, with increasing growth temperature, the C impurity concentration decreased, and it became less than the B. G. level (3 × 10^{16} cm^{-3}) at 1000 °C (Fig. 5 (c)). This is considered to be due to the combustion of hydrocarbons derived from TEGa to CO_2 with a sufficient O_2 supply, as suggested by the thermodynamic analysis [30]. In contrast, the concentration of unintentionally incorporated Si, which is a shallow-donor impurity, increased with increasing growth temperature. These results are roughly the same as those for hot-wall MOVPE-grown heteroepitaxial β-Ga_2O_3

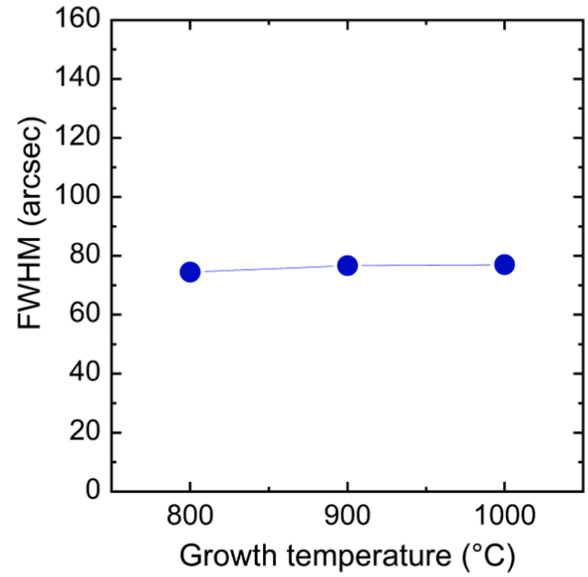

Fig. 4. Growth-temperature dependence of FWHM of XRD ω-rocking curve for unskewed asymmetric ($\bar{4}\,2\,\bar{2}$) plane with a low X-ray incident angle, measured after homoepitaxial growth at various temperatures for 1 h.

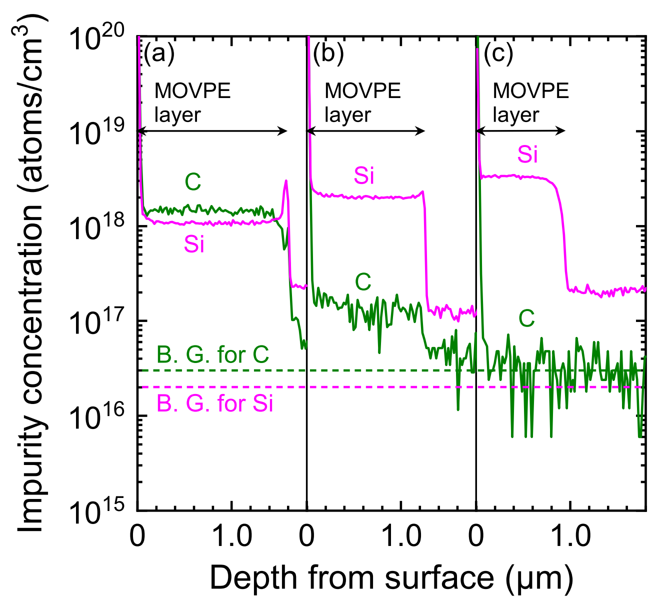

Fig. 5. SIMS depth profiles of C and Si impurity concentrations in the homoepitaxial β-Ga_2O_3 layers grown at (a) 800, (b) 900, and (c) 1000 °C. Dashed lines represent B. G. levels of the SIMS system.

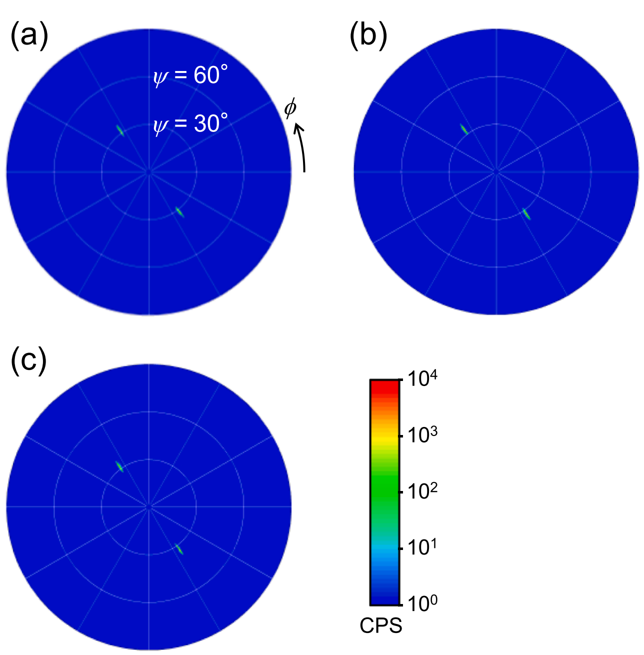

Fig. 3. XRD {1 1 1} pole figures measured after homoepitaxial growth of β-Ga_2O_3 layers for 1 h at (a) 800, (b) 900, and (c) 1000 °C. When the incident azimuth of the X-ray beam is parallel to [0 0 $\bar{1}$], ϕ is 0°; an increase in ϕ corresponds to clockwise rotation of the substrate.

layers on *c*-plane sapphire substrates [30]. The Si impurity concentration in the layers grown in this study is much higher than the Si concentration in the MOVPE-grown homoepitaxial (010) β-Ga_2O_3 layers reported by Zhang *et al* [19]. and Feng *et al* [20]. The reason for this is thought to be that the growth reactor used in this study is made of quartz glass and is a hot-wall type, so the inner wall of the reactor is etched by TEGa-derived H_2 in the system at high temperatures [35]. Suppressing the Si contamination level by changing the reactor material to a material other than quartz glass is a future challenge for hot-wall MOVPE, which is essential for achieving the intentional doping of Si in the range less than 10^{18} cm^{-3}.

The *C–V* characteristics of the vertical SBDs fabricated using the homoepitaxial layers showed that all homoepitaxial layers were n-type. Fig. 6 shows the depth profiles of $N_d - N_a$ at 300 K in the homoepitaxial β-Ga_2O_3 layers grown at various temperatures, as extracted from the *C–V* measurements conducted at 1 MHz (anode voltage range: 0 to −6 V). In the extraction, a value of 10.87 was used as the relative permittivity (ε_r) for (010) β-Ga_2O_3 [36]. The results show nearly constant depth profile of $N_d - N_a$ at each growth temperature and that, as the growth temperature increases, $N_d - N_a$ increases and the depletion-layer width at zero bias narrows. The $N_d - N_a$ values were 8.7 × 10^{17}, 2.1 × 10^{18}, and 2.9 × 10^{18} cm^{-3} in the layers grown at 800, 900, and 1000 °C, respectively; these values are similar to the unintentionally incorporated Si impurity concentration in each layer (Fig. 5). These results indicate that the carriers (electrons) in the homoepitaxial β-Ga_2O_3 layers originate from Si impurities. Notably, however, in the homoepitaxial layer grown at 800 °C, the highest concentration of impurities is C, not Si (Fig. 5(a)). Therefore, it is suggested that at least the C impurities in β-Ga_2O_3 do not behave as acceptors. Although the effect of C impurities in β-Ga_2O_3 on the optical and electrical properties is still under active debate, the results of first-principles study predict that C impurities replace Ga and become shallow or deep donors [37,38]. Detailed studies are needed in the future to conclude the state of C impurities incorporated in the β-Ga_2O_3.

4. Conclusions

The effect of the growth temperature on the growth behavior, structural quality, impurity incorporation, and electrical properties of homoepitaxial β-Ga_2O_3 layers grown by low pressure hot-wall MOVPE on (010) β-Ga_2O_3 substrates was investigated. A growth rate of ~ 1 μm/h was achieved at 800 to 1000 °C, and the growth rate decreased with increasing growth temperature. The dominant growth mode changed from 3D island growth at 800 °C to 2D step-flow growth at 1000 °C, and a homoepitaxial layer with a smooth surface was grown at 1000 °C. All the layers grown at 800 to 1000 °C were (010)-oriented single-crystalline β-Ga_2O_3 layers without twinning; a homoepitaxial layer with a high structural quality equivalent to that of the initial substrate could be grown at a growth temperature of 800–1000 °C. As the growth temperature was increased, the C impurity concentration in the homoepitaxial layer decreased, whereas the Si impurity concentration increased. The $N_d - N_a$ values for the homoepitaxial layers were nearly equal to the Si impurity concentration even when the C concentration was higher than the Si impurity concentration, which indicates that Si is the origin of the n-type carriers, and that at least C impurities are not acceptors in β-Ga_2O_3. Therefore, although investigating the suppression of Si impurity contamination in future work is important, a high growth temperature of 1000 °C is effective for the growth of smooth homoepitaxial β-Ga_2O_3 layers without C incorporation by MOVPE.

CRediT authorship contribution statement

Kazutada Ikenaga: Data curation, Formal analysis, Investigation, Visualization, Writing – original draft. **Nami Tanaka:** Data curation, Formal analysis, Investigation. **Taro Nishimura:** Data curation, Investigation. **Hirotaka Iino:** Investigation. **Ken Goto:** Data curation, Formal analysis, Investigation, Visualization. **Masato Ishikawa:** Resources. **Hideaki Machida:** Resources. **Tomo Ueno:** Resources. **Yoshinao Kumagai:** Conceptualization, Formal analysis, Funding acquisition, Methodology, Project administration, Resources, Supervision, Writing – review & editing.

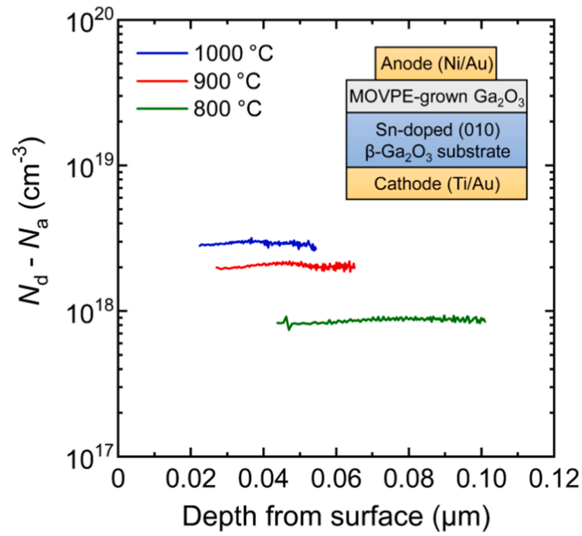

Fig. 6. Depth profiles of $N_d - N_a$ extracted from *C–V* measurements at 300 K for homoepitaxial β-Ga_2O_3 layers grown at various temperatures. The inset shows a schematic cross-sectional structure of a vertical SBD fabricated for the *C–V* measurement.

Declaration of Competing Interest

The authors declare that they have no known competing financial interests or personal relationships that could have appeared to influence the work reported in this paper.

Acknowledgments

This work was supported by Ministry of Internal Affairs and Communications (MIC) research and development (JPMI00316).

References

[1] H.H. Tippins, Phys. Rev. 140 (1965) A316.
[2] T. Onuma, S. Saito, K. Sasaki, T. Masui, T. Yamaguchi, T. Honda, M. Higashiwaki, Jpn. J. Appl. Phys. 54 (2015), 112601.
[3] M. Higashiwaki, K. Sasaki, A. Kuramata, T. Masui, S. Yamakoshi, Appl. Phys. Lett. 100 (2012), 013504.
[4] Z. Xia, H. Chandrasekar, W. Moore, C. Wang, A.J. Lee, J. McGlone, N.K. Kalarickal, A. Arehart, S. Ringel, F. Yang, S. Rajan, Appl. Phys. Lett. 115 (2019), 252104.
[5] H. Aida, K. Nishiguchi, H. Takeda, N. Aota, K. Sunakawa, Y. Yaguchi, Jpn. J. Appl. Phys. 47 (2008) 8506.
[6] A. Kuramata, K. Koshi, S. Watanabe, Y. Yamaoka, T. Masui, S. Yamakoshi, Jpn. J. Appl. Phys. 55 (2016) 1202A2.
[7] Z. Galazka, K. Irmscher, R. Uecker, R. Bertram, M. Pietsch, A. Kwasniewski, M. Naumann, T. Schulz, R. Schewski, D. Klimm, M. Bickermann, J. Cryst. Growth 404 (2014) 184.
[8] J.D. Blevins, K. Stevens, A. Lindsey, G. Foundos, L. Sande, IEEE Trans. Semicond. Manuf. 32 (2019) 466.
[9] E. Ohba, T. Kobayashi, T. Taishi, K. Hoshikawa, J. Cryst. Growth 556 (2021), 125990.
[10] K. Sasaki, A. Kuramata, T. Masui, E.G. Víllora, K. Shimamura, S. Yamakoshi, Appl. Phys. Express 5 (2012), 035502.
[11] H. Okumura, M. Kita, K. Sasaki, A. Kuramata, M. Higashiwaki, J.S. Speck, Appl. Phys. Express 7 (2014), 095501.
[12] H. Murakami, K. Nomura, K. Goto, K. Sasaki, K. Kawara, Q.T. Thieu, R. Togashi, Y. Kumagai, M. Higashiwaki, A. Kuramata, S. Yamakoshi, B. Monemar, A. Koukitu, Appl. Phys. Express 8 (2015), 015503.
[13] K. Goto, K. Konishi, H. Murakami, Y. Kumagai, B. Monemar, M. Higashiwaki, A. Kuramata, S. Yamakoshi, Thin Solid Films 666 (2018) 182.
[14] J.H. Leach, K. Udwary, J. Rumsey, G. Dodson, H. Splawn, K.R. Evans, APL Mater. 7 (2019), 022504.

[15] S. Lee, K. Kaneko, S. Fujita, Jpn. J. Appl. Phys. 55 (2016) 1202B8.
[16] H. Nishinaka, T. Nagaoka, Y. Kajita, M. Yoshimoto, Mater. Sci. Semicond. Process. 128 (2021), 105732.
[17] S. Rafique, M.R. Karim, J.M. Johnson, J. Hwang, H. Zhao, Appl. Phys. Lett. 112 (2018), 052104.
[18] M. Baldini, M. Albrecht, A. Fiedler, K. Irmscher, R. Schewski, G. Wagner, ECS J. Solid State Sci. Technol. 6 (2017) Q3040.
[19] Y. Zhang, F. Alema, A. Mauze, O.S. Koksaldi, R. Miller, A. Osinsky, J.S. Speck, APL Mater. 7 (2019), 022506.
[20] Z. Feng, A.F.M.A.U. Bhuiyan, M.R. Karim, H. Zhao, Appl. Phys. Lett. 114 (2019) 250601.
[21] K. Sasaki, D. Wakimoto, Q.T. Thieu, Y. Koishikawa, A. Kuramata, M. Higashiwaki, S. Yamakoshi, IEEE Electron Device Lett. 38 (2017) 783.
[22] J. Yang, F. Ren, M. Tadjer, S.J. Pearton, A. Kuramata, ECS J. Solid State Sci. Technol. 7 (2018) Q92.
[23] W. Li, K. Nomoto, Z. Hu, D. Jena, H.G. Xing, Appl. Phys. Express 12 (2019), 061007.
[24] C.-H. Lin, Y. Yuda, M.H. Wong, M. Sato, N. Takekawa, K. Konishi, T. Watahiki, M. Yamamuka, H. Murakami, Y. Kumagai, M. Higashiwaki, IEEE Electron Device Lett. 40 (2019) 1487.
[25] A.J. Green, K.D. Chabak, M. Baldini, N. Moser, R. Gilbert, R.C. Fitch Jr., G. Wagner, Z. Galazka, J. McCandless, A. Crespo, K. Leedy, G.H. Jessen Sr., IEEE Electron Device Lett. 38 (2017) 790.
[26] K. Sasaki, Q.T. Thieu, D. Wakimoto, Y. Koishikawa, A. Kuramata, S. Yamakoshi, Appl. Phys. Express 10 (2017), 124201.
[27] Y. Zhang, A. Neal, Z. Xia, C. Joishi, J.M. Johnson, Y. Zheng, S. Bajaj, M. Brenner, D. Dorsey, K. Chabak, G. Jessen, J. Hwang, S. Mou, J.P. Heremans, S. Rajan, Appl. Phys. Lett. 112 (2018), 173502.
[28] Z. Hu, K. Nomoto, W. Li, N. Tanen, K. Sasaki, A. Kuramata, T. Nakamura, D. Jena, H.G. Xing, IEEE Electron Device Lett. 39 (2018) 869.
[29] M.H. Wong, K. Goto, H. Murakami, Y. Kumagai, M. Higashiwaki, IEEE Electron Device Lett. 40 (2019) 431.
[30] K. Goto, K. Ikenaga, N. Tanaka, M. Ishikawa, H. Machida, Y. Kumagai, Jpn. J. Appl. Phys. 60 (2021), 045505.
[31] N. Takahashi, J. Ogasawara, A. Koukitu, J. Cryst. Growth 172 (1997) 298.
[32] E.N. Vigdorovich, Crystallogr. Rep. 50 (2005) S145.
[33] F. Alema, B. Hertog, A. Osinsky, P. Mukhopadhyay, M. Toporkov, W.V. Schoenfeld, J. Cryst. Growth 475 (2017) 77.
[34] S. Rafique, L. Han, M.J. Tadjer, J.A. Freitas Jr., N.A. Mahadik, H. Zhao, Appl. Phys. Lett. 108 (2016), 182105.
[35] K. Konishi, K. Goto, R. Togashi, H. Murakami, M. Higashiwaki, A. Kuramata, S. Yamakoshi, B. Monemar, Y. Kumagai, J. Cryst. Growth 492 (2018) 39.
[36] A. Fiedler, R. Schewski, Z. Galazka, K. Irmscher, ECS J. Solid State Sci. Technol. 8 (2019) Q3083.
[37] J.L. Lyons, D. Steiauf, A. Janotti, C.G. Van de Walle, Phys. Rev. Appl. 2 (2014), 064005.
[38] Y. Wei, T. Wang, Y. Zhang, C. Qi, J. Luan, G. Ma, H.-S. Tsai, C. Liu, M. Huo, Results Phys. 17 (2020), 103060.